

TECHNICAL  
REPORTS:  
METHODS

10.1002/2015JA021596

## Key Points:

- Spatial coverage of SuperMAG data is extended to all longitudes for latitudes 40° to the pole
- Technique uses multilinear regression, principal components and spherical cap harmonics
- Model data agree with input SuperMAG data to within statistical limits of the SuperMAG data

## Correspondence to:

C. L. Waters,  
Colin.Waters@newcastle.edu.au

## Citation:

Waters, C. L., J. W. Gjerloev, M. Dupont, and R. J. Barnes (2015), Global maps of ground magnetometer data, *J. Geophys. Res. Space Physics*, 120, 9651–9660, doi:10.1002/2015JA021596.

Received 18 JUN 2015

Accepted 4 NOV 2015

Published online 27 NOV 2015

## Global maps of ground magnetometer data

C. L. Waters<sup>1</sup>, J. W. Gjerloev<sup>2,3</sup>, M. Dupont<sup>1</sup>, and R. J. Barnes<sup>2</sup>

<sup>1</sup>School of Mathematical and Physical Sciences, University of Newcastle, Callaghan, New South Wales, Australia, <sup>2</sup>The Johns Hopkins University Applied Physics Laboratory, Laurel, Maryland, USA, <sup>3</sup>Birkeland Centre of Excellence, University of Bergen, Bergen, Norway

**Abstract** A statistical-based method combined with basis function expansion techniques is described in order to provide extensive maps of the ground level perturbation magnetic field from 40° magnetic latitude to the north magnetic pole for all longitudes. The method combines historical data from the SuperMAG data base, Principal Component Analysis, and a spherical cap harmonic basis function expansion in order to fill in magnetic perturbation data where there are no magnetometers and produce the poloidal current potential. The maps have a regular grid with a 2° latitude and 1 h longitude spacing. The statistical process uses SuperMAG data derived magnetic indices plus the solar zenith angle which orders the resulting spatial maps by geomagnetic activity indicators to enhance model agreement with the data. For quiet through to moderate magnetic activity intervals, the root-mean-square error between the input and the fitted data are 18 nT and 10 nT for the north-south and east-west components, respectively, which are of similar magnitude to the statistical uncertainty in the SuperMAG data set.

## 1. Introduction

Ground-based magnetometer data have provided fundamental information on auroral processes since the early 1900s. While the association between magnetic field variations and auroral activity was recognized as early as the mid-1700s, the work of Birkeland (1908) yielded the first estimates of the polar region electric current patterns using data obtained from ground magnetometer measurements. Since then, as pointed out by Gjerloev [2012], ground magnetometer data have been pivotal for magnetosphere-ionosphere studies including substorm properties and dynamics, connections between solar wind variability and ionospheric currents, auroral dynamics and ionosphere electrojet systems. These are considered “global” phenomena and their study requires measurements at degree-scale spatial resolution (at least in latitude) and minute temporal intervals. This paper is concerned with obtaining comprehensive, ground level magnetic field signatures of electric currents flowing in the auroral ionosphere.

Magnetosphere-ionosphere energy coupling involves large spatial scale processes which has motivated the establishment of magnetometer arrays. A number of two-dimensional magnetometer arrays were installed during the International Magnetospheric Study (IMS; 1976–1979) in order to deduce properties of the source current systems [e.g., Untiedt and Baumjohann, 1993]. After extracting the vector magnetic field components due to external currents, the data were often represented as equivalent current maps using the horizontal magnetic field components, which led to methods that separate the divergence-free and curl-free parts of the magnetic field and ionospheric current systems [Kamide et al., 1981; Akasofu et al., 1981].

It was soon realized that electrical properties of the ionosphere over the auroral zone might be deduced from ground magnetometer measurements. Kamide and Richmond [1982] used data from the IMS Alaskan magnetometer array to investigate the influence of different ionospheric conductance models on the current systems derived from ground magnetometer observations. In order to achieve the required spatial coverage, the data were averaged in magnetic local time (MLT) bins, thus trading off spatial for temporal information. Maps of electrodynamic parameters were obtained over all MLT and from 60° to the pole using spherical harmonic basis function expansion methods.

Ground magnetometer data obtained from any 2-D spatial array is insufficient to uniquely determine the ionospheric current geometry. Additional information such as ionosphere conductance or satellite measurements are required. This means that ground magnetic perturbation signatures can be estimated if information on electrodynamic properties of the ionosphere are available. For example, assuming a constant Pedersen to Hall

conductance ratio and statistical models of the ionospheric electric and magnetic potential, *Weimer* [2005] compared two methods for estimating the large-scale, long-period ground-level geomagnetic variations. The temporal resolution of such data was improved by *Green* [2006] and *Green et al.* [2007] who folded in electric field patterns obtained from the Super Dual Auroral Radar Network (SuperDARN). A disadvantage of this approach is the dependence on ionosphere conductance properties that are not well known on suitable spatial and temporal scales.

Ground magnetic field measurements at minute cadence over limited regions have been available for many decades. However, the difficulty is to provide such data over a global spatial extent. Research efforts in both the geophysics and space physics communities have forged international collaborations that allow data exchange among separated magnetometer arrays. For example, during the 1980s the International Real-time Magnetic Observatory Network (INTERMAGNET) was established, which aims to deliver global magnetic field data.

SuperMAG is a more recent international collaborative effort designed to provide global, ground-based magnetic field data at 1 min cadence with a focus on magnetosphere-ionosphere research [*Gjerloev*, 2012]. The SuperMAG initiative represents state-of-the-art data preprocessing and delivery, allowing easy access to magnetometer data from over 300 locations around the world in a common format and with best practice applied in order to remove data anomalies. While the number of magnetometer stations has increased since the 1980s, the instrumentation is confined to available land. Therefore, obtaining estimates of global ground magnetometer signatures with degree-scale spatial resolution in longitude remains a challenge.

## 2. Extending SuperMAG Data Spatial Coverage

Given a sparse and irregularly spaced distribution of magnetometer data over Earth's surface, the objective is to provide estimates of these data at locations where instrumentation is absent. The standard procedure in geophysics is to employ a basis function expansion using spherical harmonic functions, keeping the order sufficiently small in order to avoid aliasing in areas of sparse data coverage [*Chapman and Bartels*, 1940]. Magnetometer arrays in both latitude and longitude configurations have typical spacings of  $1^{\circ}$ – $2^{\circ}$  in latitude and subhour spacing in MLT over limited areas. Since the perturbation fields detected by ground magnetometers sense magnetic effects of ionospheric currents integrated over an area of order  $\approx 200$  km, a spacing of  $2^{\circ}$  is the target latitude separation [*Ponomarenko et al.*, 2001].

The resolution in MLT is often less stringent, given that typical longitudinal structures of the large-scale ionosphere current systems in the auroral regions are larger than the latitude spatial scales. While specific spatial patterns of the auroral current systems vary with solar and geomagnetic activity, the current systems tend to align with the geometry of the space environment while Earth rotates beneath. Therefore, for a given latitude distribution of sensors on Earth's surface, information is available at all local times at least once per day, albeit at different times.

A direct approach for estimating physical values over some discrete latitude and MLT grid is to bin all available data by parameters that might be considered "drivers" of the system. For example, the SuperDARN data processing bins ionospheric Doppler velocity values by Interplanetary Magnetic Field (IMF) magnitude and geometry in order to construct statistical convection patterns which are then used to fill in spatial data gaps for a given UT, followed by basis function fitting [*Ruohoniemi and Baker*, 1998]. This approach assumes adequate specification of the system through identification and selection of relevant drivers that are keyed to unique system states. In particular, assumptions of this approach include (i) the IMF variations measured at the L1 Lagrangian point (e.g., at the ACE spacecraft) propagate toward Earth as a plane wave with no in-plane structure, (ii) internal magnetosphere processes are excluded, (iii) there is no delay between IMF "cause" and any effects on the system, (iv) states of the system are uniquely characterized by the IMF, (v) there is no filtering of the driver so that a "spike" in the IMF data can give a different system state, and (vi) there is no information included that is related to the history of the magnetosphere-ionosphere system.

Statistical regression methods can also be applied to these types of problems. This approach can provide more information on the data estimation process including estimates of uncertainties and cross-correlation details compared with the driver binning approach. Examples include multilinear regression (MLR) using least squares fit criterion and Bayesian regression methods. For the SuperMAG data, we have employed the MLR-least squares fit approach coupled with Principal Component Analysis (PCA). This method is known as

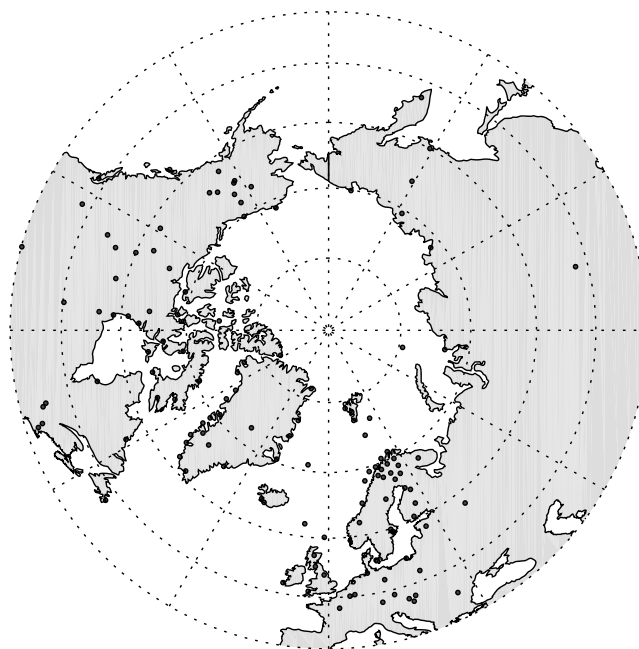


**Figure 1.** Locations of the magnetometers used to provide the SuperMAG data for 2001.

[Gjerloev, 2012]. A local, orthogonal magnetic coordinate system is used where the component values are  $B_N$  positive in the local magnetic north direction,  $B_E$  is positive magnetic eastward, and positive  $B_Z$  points vertically downward. Locations of the available magnetometers for 2001 are shown in Figure 1.

The selection of model parameters is more involved. One approach is to follow the SuperDARN method, choosing solar wind parameters that might order the ground magnetometer data. This would require unraveling links between parameters obtained outside the magnetosphere such as solar wind velocities and interplanetary magnetic field (IMF) components [Arnoldy, 1971; Weigel *et al.*, 2003], IMF clock and cone angles, dynamic pressure and energy coupling functions [Newell *et al.*, 2007], accounting for the transition of energy through the magnetosphere, and ionosphere with associated ionosphere conductance effects.

Based on this approach, a multilinear regression (MLR) model was attempted that used over 50 parameters involving solar wind properties, functions of these variables, and magnetic indices. This exercise highlighted two main difficulties. The first involved adverse consequences of using a large number of parameters in a statistical model which can cause overfitting of the data [Burnham and Anderson, 2002]. Second, any cause-effect pathways between the ground perturbation magnetic signatures and parameters measured in the solar wind will most certainly have time delays, and these may not necessarily be the same over all latitudes and MLT. While time lags can be accounted for in more sophisticated models, this complication can be avoided if time-lagged data (e.g., solar wind measurements) are excluded. Such a simpler approach is described below, given that the aim is to provide uniform gridded coverage without attempting to discern causal relationships.

Our approach was to confine selection of the model parameters to data products derived from the ground magnetometer data. Specifically, there are several magnetic indices that are derived from ground observations at minute time cadence. Newell and Gjerloev [2011a] used data from magnetometer arrays that collaborate with SuperMAG to derive the SME = SMU – SML indices. These are a generalization of the auroral electrojet indices calculated from 100 or more sites instead of the 12 used in the International Association of Geomagnetism and Aeronomy (IAGA) auroral electrojet indices,  $AE(12) = AU(12) - AL(12)$ . Newell and Gjerloev [2011b] showed that there are three advantages to including more stations: (i) improved timing of auroral events, (ii) improved knowledge of event location, and (iii) improved measures of event intensity. These improvements are a result of the additional number of stations distributed in MLT which increases the probability of a station being in the right location at the right time.

Principal Component Regression (PCR) [e.g., Burnham and Anderson, 2002]. The drivers of linear models are chosen from a set of magnetic indices in order to avoid difficulties with using solar wind variables. The PCR process fills in spatial data gaps, allowing subsequent high-order spherical cap harmonic analysis (SCHA). The potential functions obtained from the SCHA may then be used with SuperDARN and satellite data from the Active Magnetosphere and Planetary Electrodynamics Response Experiment to give estimates of the ionosphere conductance [Green *et al.*, 2007].

### 3. Experimental Data

The ground magnetometer data are at 1 min cadence and were obtained from the SuperMAG database, where the contributed magnetometer data are processed and stored in a common format

**Table 1.** List of Regression Model Parameters

Model Parameter	Description
SML	SuperMAG auroral AL index
SMU	SuperMAG auroral AU index
SML_s	SML for sunlit locations
SMU_s	SMU for sunlit locations
SML_d	SML for dark locations
SMU_d	SMU for dark locations
SMR00, SMR06, SMR12, and SMR18	SuperMAG partial ring current indices
<i>SYM-H</i> and <i>SYM-D</i>	IAGA defined ring current indices
<i>ASYM-H</i> and <i>ASYM-D</i>	IAGA asymmetric ring current indices
Solar zenith angle	Solar zenith angle (degrees)
PC	Polar cap magnetic index

The *SYM-H* index can be regarded as a 1 min version of the hourly *Dst* index [Wanliss and Showalter, 2006]. Newell and Gjerloev [2012] used the SuperMAG data to introduce partial ring current indices. These are labeled SMR-00, SMR-06, SMR-12, and SMR-18 for their center local time range. These indices incorporate data from 98 midlatitude and low latitude stations. Newell and Gjerloev [2012] concluded that the SMR-local time indices showed large differences during the evolution of a magnetic storm and only came back to the same values at the latter stages of the recovery phase. This indicates that the assumption of a symmetric ring current, on which the *SYM-H* and *Dst* indices are based, is questionable for the main phase and early recovery phase of magnetic storms. Both the SME and the SMR indices used in this study were downloaded from the SuperMAG website. At higher latitudes, the polar cap magnetic index (PC) may be used. This index is derived from stations located at Thule and Vostok and may be downloaded from <http://pc-index.org>. At present, there is no SuperMAG analog for PC. The choice of model parameters used in the PCA and multilinear regression process are listed in Table 1.

#### 4. Principal Component Regression Model

Given a time series of ground magnetic field data and a set of model parameters (magnetic indices and solar zenith angle), a linear model is

$$y_i = \beta_0 + \beta_1 x_{1i} + \dots + \beta_k x_{ki} + \epsilon_i \quad (i = 1, \dots, n) \quad (1)$$

For Principal Component Regression (PCR) the  $y_i$  are the perturbation magnetic field  $dB_N$ ,  $dB_E$ , and  $dB_Z$  values from SuperMAG. The  $x_{ki}$  are eigenvectors of the covariance matrix derived from the magnetic indices and solar zenith angle values that represent the independent variables,  $\beta_k$  are the regression coefficients, and  $\epsilon_i$  are the model errors, assumed to have zero mean. In matrix form

$$\mathbf{y} = \mathbf{X}\boldsymbol{\beta} + \boldsymbol{\epsilon} \quad (2)$$

and the usual least squared estimate for  $\boldsymbol{\beta}$  is

$$\hat{\boldsymbol{\beta}} = (\mathbf{X}^T \mathbf{X})^{-1} \mathbf{X}^T \mathbf{y} \quad (3)$$

In the usual multilinear regression (MLR) process, the magnetic indices, and solar zenith angle values would be directly used as the  $x_{ki}$  in equation (1). For PCR, the magnetometer data are regressed onto a set of eigenvectors derived from the covariance matrix. In detail, the procedure is as follows:

1. The magnetic indices and solar zenith angle data over a given year were sorted into 3 min wide MLT windows.
2. For each 3 min wide MLT bin, each variable was standardized (subtract the mean, divide by the standard deviation).
3. These data were used to calculate the covariance matrix and since the data are standardized, the covariance matrix is identical to the correlation matrix.

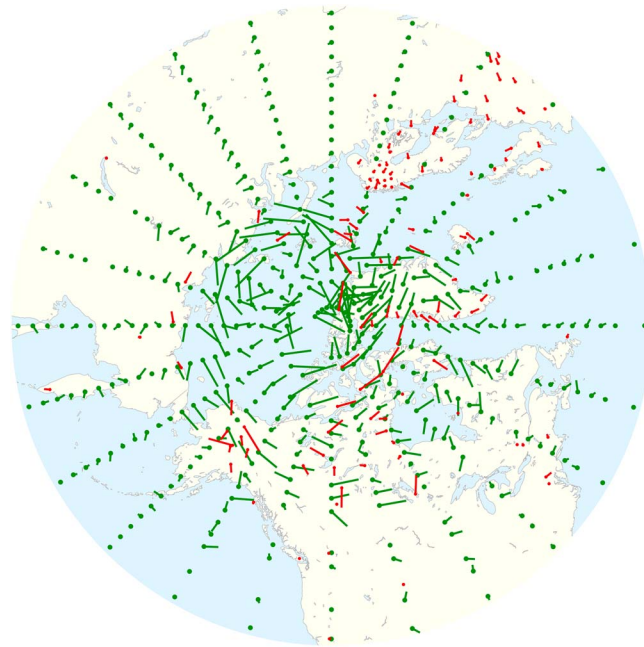


**Figure 2.** Data and output from the PCR model for 0830 UT, 24 May 2001. The data from all SuperMAG stations are shown in red. The PCR model gave the green vectors.

4. The eigenvectors and eigenvalues of this correlation matrix were computed. For  $p$  variables used to construct the correlation matrix, there are  $p$  orthogonal eigenvectors, each being a linear combination of the standardized magnetic indices and solar zenith angle values. The percentage variance explained by  $k$  of these  $p$  eigenvectors ( $k \leq p$ ) and associated eigenvalues,  $\lambda_k$  is

$$\frac{\lambda_1 + \lambda_2 + \dots + \lambda_k}{\lambda_1 + \lambda_2 + \lambda_3 \dots \lambda_{p-1} + \lambda_p} \times 100\% \quad (4)$$

where the denominator is the sum of all eigenvalues. The eigenvectors were sorted according to the magnitudes of the eigenvalues.

5. Equation (4) was used to select the  $k$  eigenvectors required to achieve a statistical confidence level of 99%.
6. Each component (e.g.,  $dB_N$ ) of the MLT binned magnetometer data were regressed onto these  $k$  eigenvectors to give the regression coefficients,  $\beta$ , as described by equation (3).

The north-south ( $dB_N$ ), east-west ( $dB_E$ ), and vertical ( $dB_Z$ ) components of the perturbation magnetometer data from all available stations in the  $40^\circ - 90^\circ$  latitude range for a full year were used. The magnetic indices and solar zenith angle values were obtained for the same UT times, allowing for the solar zenith angle to vary with magnetometer location and time. This gave a linear model with 16 possible parameters which are given in Table 1. If any parameter value was missing then the whole data record for that time was discarded. The number of data records discarded depends on the year and the station. For 2001, 136 stations provided data and 110 stations had over 80% availability.

The 3 min wide MLT bin was stepped by 1 min intervals through 24 h of MLT. This process yielded 1440 sets of regression coefficients for each station, keyed to each MLT minute of the 24 h of MLT. Using these coefficients, the model  $dB_N$ ,  $dB_E$ , and  $dB_Z$  were calculated for all MLT. This provided PCR model perturbation magnetic field values for all MLT in 1 min steps and with a latitude spacing of  $2^\circ$ .

## 5. Results

An example map of vector ( $dB_N$  and  $dB_E$ ) data for a quiet interval ( $Kp = 1$ ) is shown in Figure 2. The vectors have been rotated by  $90^\circ$  to more clearly demonstrate the link between the ground fields and the ionospheric plasma convection pattern. For a given UT, the input SuperMAG observations are at specific locations on a magnetic latitude (MLat), MLT map, as shown in red. In a number of cases, there are multiple stations in the

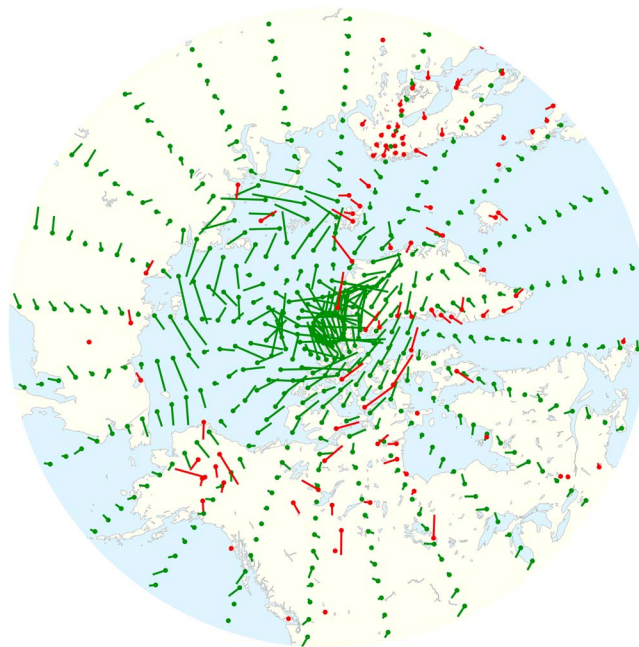


**Figure 3.** Perturbation magnetic field vectors obtained from a spherical cap harmonic expansion of the SuperMAG magnetic field data for 0830 UT, 24 May 2001. The input SuperMAG data are shown in red.

for spherical cap harmonics have noninteger eigenvalues from the Legendre differential equation, which depend on the imposed boundary conditions. A method to generate these basis functions to high order and for both Dirichlet and Neumann boundary conditions was described by *Ogburn et al.* [2014] and used previously by *Waters et al.* [2001] and *Waters and Sciffer* [2008].

The  $dB_N$  and  $dB_E$  magnetic perturbation data shown in Figure 2 were input to a basis function expansion process that used vector spherical harmonic cap functions. The magnetic field data included the experimental values obtained from SuperMAG in addition to the PCR model values at locations where magnetometers were absent. The basis function expansion allows for different weightings to be applied on the SuperMAG compared with the PCR model magnetic field values. In this work, both data sets have a weighting of unity. The maximum latitude extent was  $50^\circ$  with the largest spherical cap eigenvalue chosen to give  $2^\circ$  latitude resolution and azimuthal wave number,  $m = 5$ . The fitted data (rotated by  $90^\circ$ ) are shown in Figure 3. For the input data, the (min;max) of the  $dB_N$  component was  $(-91;116)$  nT while the (min;max) of the  $dB_E$  component was  $(-68;100)$  nT. Comparison of Figures 2 and 3 shows that the input and spherical cap basis function fitted data are very similar. An estimate of how similar, or the quality of the fit, may be obtained from the root-mean-square error (RMSE) calculated using the input and fitted data at the locations of the input data. These RMSE values were (18;10) nT for  $(dB_N;dB_E)$  components.

## 6. Discussion

Figures 2 and 3 show that a multilinear regression model that uses indices derived from ground magnetometer data may be used to fill in magnetic perturbation values to obtain a more global data set. This approach does not provide cause and effect information for the ground magnetometer data in a way that a solar wind based, parameter model might do. However, the magnetic index-based approach is more direct and simple and avoids difficulties with time delays between possible solar wind drivers and the ground signatures and unknown ionospheric conductance effects.

Any process that uses a mixture of experimental data supported by statistical methods to infer additional data values requires an assessment of the goodness of fit. The usual root-mean-square error (RMSE) metric was used to quantify deviations of the PCR model outputs from the input experimental data values. However, the PCR model performance depends on the choice of parameters to include which is related to the methodology used to assess which parameters might be relevant. Table 1 lists the parameters that might be included. After

same  $2^\circ$  wide latitude ring. A half-cosine weighting function was used to transition data in the same latitude ring so that the PCR model data were always determined from the closest experimental input values.

The combined experimental and PCR model  $dB$  data for a given UT may be used in an orthogonal, basis function expansion process. This facilitates studies of electrodynamic properties of the ionosphere by providing magnetic potential functions derived from the ground data as described by *Green et al.* [2007]. Spherical cap harmonic basis functions are closely related to the more commonly used spherical harmonic functions, which are the surface solutions to the Laplace equation over a full sphere [*Haines, 1985*]. The longitudinal solutions are the same, being functions of  $\sin(m\phi)$  and  $\cos(m\phi)$ , where  $m$  is an integer that specifies the longitudinal wavelength. The solutions in latitude

the chosen parameter data, over a given time period (e.g., years), are standardized, the correlation matrix reveals how each parameter is related (or correlated) to all others in the set. For example, the *SYM-H* index showed correlation coefficients of  $\rho > 0.95$  with all the SuperMAG partial ring current indices (SMR00, SMR06, etc.). SMU is similar to SMU<sub>s</sub> ( $\rho = 0.98$ ) and similarly for SML and SML<sub>s</sub> ( $\rho = 0.9$ ). This suggests that SML, SMU, and *SYM-H* can be deleted from the model parameters as any influence they might have would be taken care of by the remaining parameters.

A direct process of parameter choice, based only on the linear correlation coefficient, may be inappropriate for all parameters. The correlation coefficients for all combinations of SMR00, SMR06, SMR12, and SMR18 were  $\rho > 0.9$ , meaning that on average, these are highly correlated parameters. These were all retained in the model parameter list since they can become less dependent during intervals of enhanced magnetic activity, as discussed by *Newell and Gjerloev* [2012]. For the 24 May 2001 event shown in Figure 2, including all 16 parameters, gave RMSE values of (33;29) nT for the ( $dB_N; dB_E$ ) component data. Excluding the polar cap index gave RMSE values of (34;27) nT.

The SuperMAG auroral indices SMU and SML may be combined to form SME = SMU – SML along with their sunlit and dark ionosphere versions. The minimum RMSE values were obtained for a PCR model that only used SME, SME<sub>s</sub>, and SME<sub>d</sub>; the four partial ring current indices; and solar zenith angles; giving a RMSE = (29;25) nT. Ten PCR models were trialed, using different combinations that included and then excluded the polar cap index, *SYM-H* and *SYM-D*, *ASYM-H*, and *ASYM-D*, and changing SMU<sub>s</sub> for SME. Over these different models, the RMSE values only varied by 5 nT.

The choice of parameters to include was therefore informed by correlation analyses in addition to consideration of parameters that might be expected to improve the solution. Some dependence on MLT is provided by the SMR00–SMR18 indices. The latitude and MLT dependence of the PCR model goodness of fit for all SuperMAG data over 2001 is shown in Figure 4. One region for improvement, common to all three magnetic field components, is the dayside polar cap which would benefit from additional magnetometer data in addition to further research on parameters that might account for the cusp region. For  $dB_N$  and  $dB_Z$ , the RMSE are larger around the auroral zone. However, the larger RMSE values are consistent with the ground magnetometer values which are generally larger there. The choice of parameters might be further refined by taking narrower ranges in latitude that target known processes at midlatitude, auroral latitude, and high latitude, in addition to the development of indices that are more focused on specific components of the magnetometer data. Any future refinements will be described and the refined data made available from the SuperMAG web sites (<http://supermag.jhuapl.edu> and <http://supermag.uib.no>).

The PCR model is useful for adding data in order to constrain high-order, spherical harmonic basis function-based fits to the ground magnetometer data. The basis function sum is directly related to the poloidal potential used for M-I coupling studies [*Green et al.*, 2007]. Figure 3 shows the results of such a data fit for a magnetically quiet case. For these spherical harmonic cap fitted data, the RMSE values were (18;10) nT for the ( $dB_N; dB_E$ ) magnetic field components. The expected uncertainties for the SuperMAG data as a whole were defined and discussed by *Gjerloev* [2012]. Their estimates of the full width, half maximum values are similar to the RMSE values obtained from the basis function expansion fit. Therefore, our method provides perturbation magnetometer data with an accuracy that approaches statistical limitations of the SuperMAG data set.

Global maps of the ground magnetic field perturbations are invaluable for studies of magnetosphere-ionosphere coupling. The more interesting cases involve transitions of the magnetosphere from relatively quiet to more active states. A  $Kp_{\max} = 7$  storm that was associated with a southward turning ( $B_z$  of  $-15$  nT) of the IMF occurred around 0320 UT, 28 October 2001. While the IMF  $B_x$  component remained small, the  $B_y$  component jumped to values up to 15 nT. This represents a challenging case for any statistical model.

A sequence of four maps of the horizontal components of the ground magnetometer data for 0300–0330 UT, 28 October 2001, are shown in Figure 5. The red arrows show the input ( $dB_N; dB_E$ ) components from SuperMAG. The green arrows show the results from the spherical cap harmonic fit to the input and PCR model data. All vectors have been rotated by 90°. Over the 0300–0320 UT interval, there was moderate magnetic activity ( $Kp = 3$ ), with IMF  $B_z \approx -4$  nT and  $B_y \approx +5$  nT. Figure 5 shows good agreement between the input SuperMAG data and the fitted vectors. Figure 5d shows the enhanced activity pattern, which is consistent with the positive IMF  $B_y$ . The spherical cap expansion process uses a magnetic potential useful in

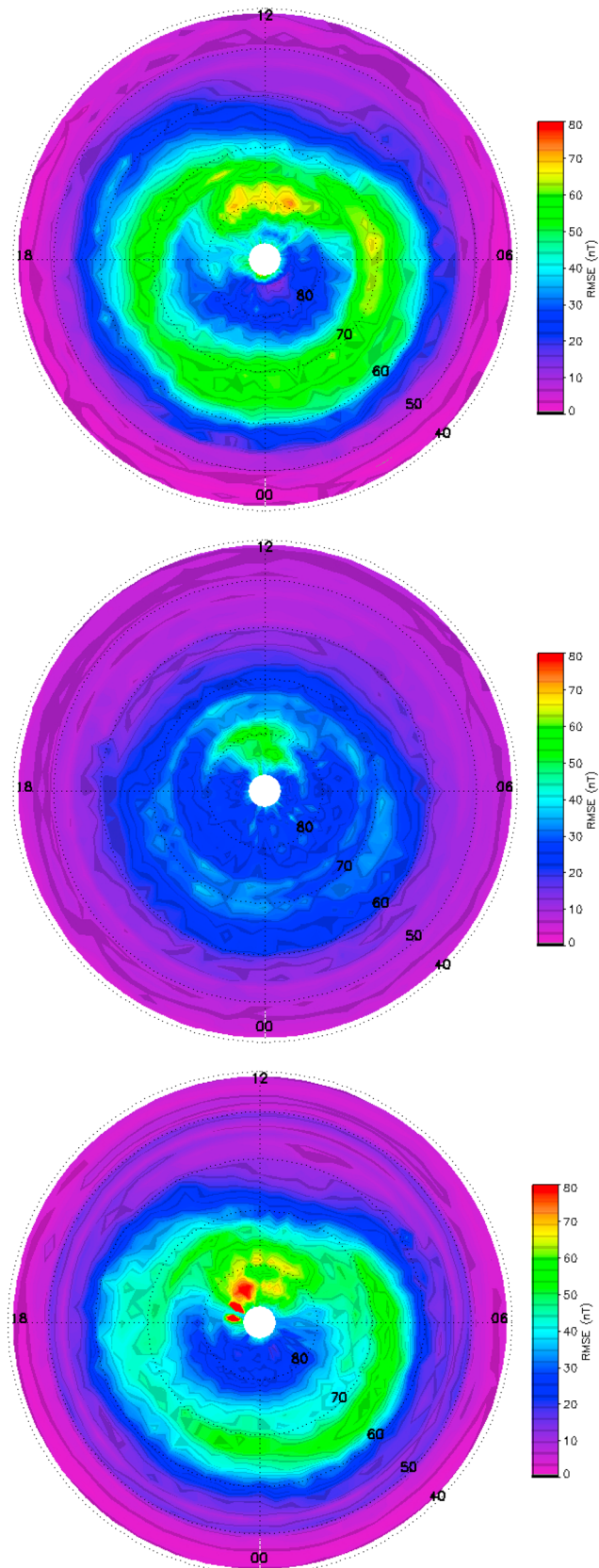


**Figure 4.** Root-mean-square error (RMSE) values for all 2001 data using an PCR model with 1 min cadence. The RMSE for north-south (top), east-west (center), and vertical (bottom) components of the perturbation magnetic field data.

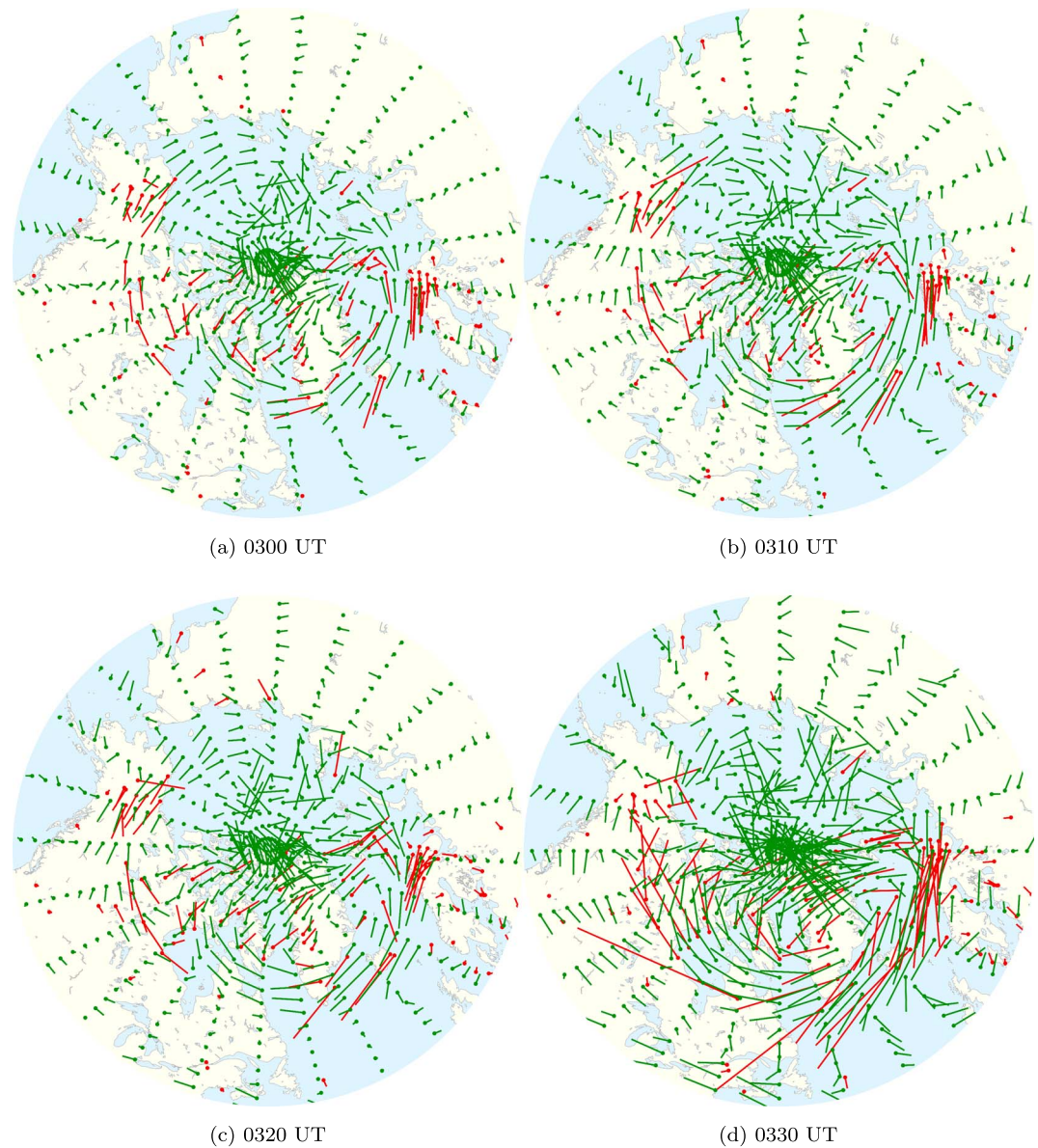


**Figure 5.** Sequence of maps of the horizontal components of the ground magnetometer data for 0300–0330 UT, 28 October 2001. The red arrows show the input data from SuperMAG, while the green arrows are from the spherical cap basis function fit.

magnetosphere-ionosphere coupling studies when the divergence and curl free parts are required. The PCR based data modeling described here facilitates obtaining these solutions over  $40^{\circ}$ – $90^{\circ}$  latitude and all MLT.

## 7. Conclusion

Perturbation magnetic field data over all MLT and from mid to high latitudes at minute time cadence are desirable for global studies of magnetosphere-ionosphere coupling. While the number of operational magnetometers has increased over recent years, the experimental data are ultimately limited by land availability. In order to pursue high spatial resolution information from ground magnetometer data, a PCR model has been described that may be used to fill in ground magnetometer data in order to constrain spherical harmonic basis function-based fitting. Assisted by the PCR model, the goodness of fit, based on the RMSE calculated from the input magnetometer data and the spherical cap fitted data, is of similar magnitude as the statistical uncertainties in the SuperMAG data set.

The PCR model is based on parameters that are useful for extending spatial coverage rather than attempting to untangle causal relationships between solar wind parameters and auroral current systems. SuperMAG data derived indices are used in order to capture MLT variability in more detail compared with the IAGA defined values. This has highlighted some need for development of suitable parameters that capture cusp dynamics and those that have a greater dependence on the ground magnetometer  $dB_z$  component. The horizontal magnetic field components are normally used in magnetosphere-ionosphere studies, and the approach described provides estimates of these components at  $2^\circ$  latitude resolution, for all MLT and for quiet and active magnetic conditions.

#### Acknowledgments

For the ground magnetometer data we gratefully acknowledge the following: Intermagnet; USGS, Jeffrey J. Love; CARISMA and PI Ian Mann; CANMOS; the S-RAMP Database, PI K. Yumoto, and K. Shiokawa; The SPIDR database; AARI, PI Oleg Troshichev; The MACCS program, PI M. Engebretson, Geomagnetism Unit of the Geological Survey of Canada; GIMA; MEASURE, UCLA IGPP, and Florida Institute of Technology; SAMBA, PI Eftyhia Zesta; 210 Chain, PI K. Yumoto; SAMNET, PI Farideh Honary; the institutes who maintain the IMAGE magnetometer array, PI Eija Tanskanen; PENGUIN; AUTUMN, PI Martin Connors; DTU Space, PI Jürgen Matzka; South Pole and McMurdo Magnetometer, PI's Louis J. Lanzarotti and Alan T. Weatherwax; ICESTAR; RAPIDMAG; PENGUIN; British Antarctic Survey; McMac, PI Peter Chi; BGS, PI Susan Macmillan; Pushkov Institute of Terrestrial Magnetism, Ionosphere and Radio Wave Propagation (IZMIRAN); GFZ, PI Jürgen Matzka; MFGI, PI B. Heilig; IGFPAS, PI J. Reda; University of LAquila, PI M. Vellante; and SuperMAG, PI Jesper W. Gjerloev. Data used in this study are available from the SuperMAG web site (<http://supermag.jhuapl.edu> and <http://supermag.uib.no>).

#### References

- Akasofu, S.-I., Y. Kamide, and J. Kisabeth (1981), Comparison of two modeling methods for three-dimensional current systems, *J. Geophys. Res.*, *86*, 3389–3396, doi:10.1029/JA086iA05p03389.
- Arnoldy, R. L. (1971), Signature in the interplanetary medium for substorms, *J. Geophys. Res.*, *76*, 5189–5201, doi:10.1029/JA076i022p05189.
- Burnham, K., and D. Anderson (2002), *Model Selection and Multimodel Inference: A Practical Information-Theoretic Approach*, Springer, New York.
- Chapman, S., and J. Bartels (1940), *Geomagnetism*, vol. 2, Oxford Univ. Press, Amen House, London.
- Gjerloev, J. (2012), The SuperMAG data processing technique, *J. Geophys. Res.*, *117*, A09213, doi:10.1029/2012JA017683.
- Green, D. L. (2006), The use of spherical cap harmonic analysis in predicting ground magnetic perturbations from ionospheric electric field and conductance models, paper presented at Australian Institute of Physics 17th National Congress 2006, Brisbane, 3–8 Dec.
- Green, D. L., C. L. Waters, H. Korth, B. J. Anderson, A. J. Ridley, and R. J. Barnes (2007), Technique: Large-scale ionospheric conductance estimated from combined satellite and ground-based electromagnetic data, *J. Geophys. Res.*, *112*, A05303, doi:10.1029/2006JA012069.
- Haines, G. V. (1985), Spherical cap harmonic analysis, *J. Geophys. Res.*, *90*, 2583–2591, doi:10.1029/JB090iB03p02583.
- Kamide, Y., and A. D. Richmond (1982), Ionospheric conductivity dependence of electric fields and currents estimated from ground magnetic observations, *J. Geophys. Res.*, *87*, 8331–8337, doi:10.1029/JA097iA10p08331.
- Kamide, Y., A. D. Richmond, and S. Matsushita (1981), Estimation of ionospheric electric fields, ionospheric currents, and field-aligned currents from ground magnetic records, *J. Geophys. Res.*, *86*, 801–813, doi:10.1029/JA086iA02p00801.
- Newell, P. T., and J. W. Gjerloev (2011a), Evaluation of SuperMAG auroral electrojet indices as indicators of substorms and auroral power, *J. Geophys. Res.*, *116*, A12211, doi:10.1029/2011JA016779.
- Newell, P. T., and J. W. Gjerloev (2011b), Substorm and magnetosphere characteristic scales inferred from the SuperMAG auroral electrojet indices, *J. Geophys. Res.*, *116*, A12232, doi:10.1029/2011JA016936.
- Newell, P. T., and J. W. Gjerloev (2012), SuperMAG-based partial ring current indices, *J. Geophys. Res.*, *117*, A05215, doi:10.1029/2012JA017586.
- Newell, P. T., T. Sotirelis, K. Liou, C.-I. Meng, and F. J. Rich (2007), A nearly universal solar wind-magnetosphere coupling function inferred from 10 magnetospheric state variables, *J. Geophys. Res.*, *112*, A01206, doi:10.1029/2006JA012015.
- Ogburn, D. X., C. L. Waters, M. D. Sciffer, J. A. Hogan, and P. C. Abbott (2014), A finite difference construction of the spheroidal wave functions, *Comput. Phys. Commun.*, *185*, 244–253, doi:10.1016/j.cpc.2013.07.024.
- Ponomarenko, P. V., C. L. Waters, M. D. Sciffer, B. J. Fraser, and J. C. Samson (2001), Spatial structure of ULF waves: Comparison of magnetometer and Super Dual Auroral Radar Network data, *J. Geophys. Res.*, *106*, 10,509–10,517, doi:10.1029/2000JA000281.
- Ruohoniemi, J. M., and K. B. Baker (1998), Large-scale imaging of high-latitude convection with Super Dual Auroral Radar Network HF radar observations, *J. Geophys. Res.*, *103*, 20,797–20,811, doi:10.1029/98JA01288.
- Untiedt, J., and W. Baumjohann (1993), Studies of polar current systems using the IMS Scandinavian magnetometer array, *Space Sci. Rev.*, *63*, 245–390.
- Wanliss, J. A., and K. M. Showalter (2006), High-resolution global storm index: Dst versus SYM-H, *J. Geophys. Res.*, *111*, A02202, doi:10.1029/2005JA011034.
- Waters, C. L., and M. D. Sciffer (2008), Field line resonant frequencies and ionospheric conductance: Results from a 2-D MHD model, *J. Geophys. Res.*, *113*, A05219, doi:10.1029/2007JA012822.
- Waters, C. L., B. J. Anderson, and K. Liou (2001), Estimation of global field aligned currents using the Iridium system magnetometer data, *Geophys. Res. Lett.*, *28*, 2165–2168, doi:10.1029/2000GL012725.
- Weigel, R. S., A. J. Klimas, and D. Vassiliadis (2003), Solar wind coupling to and predictability of ground magnetic fields and their time derivatives, *J. Geophys. Res.*, *108*(A7), 1298, doi:10.1029/2002JA009627.
- Weimer, D. R. (2005), Predicting surface geomagnetic variations using ionospheric electrodynamic models, *J. Geophys. Res.*, *110*, A12307, doi:10.1029/2005JA011270.